Progress in Organic Coatings 101 (2016) 331–341

Contents lists available at ScienceDirect

Progress in Organic Coatings

journal homepage: www.elsevier.com/locate/porgcoat

Corrosion protection of carbon steel by solvent free epoxy coating containing hydrotalcites intercalated with different organic corrosion inhibitors

Nguyen Thuy Duong[a,b], To Thi Xuan Hang[a], Arnaud Nicolay[b], Yoann Paint[c], Marie-Georges Olivier[b,c,*]

[a] Institute for Tropical Technology, Vietnam Academy of Science and Technology, 18 Hoang Quoc Viet, Cau Giay, Hanoï, Vietnam
[b] Université de Mons (UMONS), Faculty of Engineering, Materials Science Department, 20 Place du Parc, Mons, Belgium
[c] Materia Nova Research Center, Parc Initialis, Avenue Copernic, Mons, Belgium

ARTICLE INFO

Article history:
Received 19 February 2016
Received in revised form 1 July 2016
Accepted 2 August 2016
Available online 13 September 2016

Keywords:
Solvent free epoxy coatings
Hydrotalcites
Organic corrosion inhibitor
Electrochemical impedance spectroscopy
Suspension stability

ABSTRACT

Hydrotalcites intercalated with two different corrosion inhibitors: 2-benzothiazolythio-succinic acid (BTSA) and benzoate (BZ) were prepared by coprecipitation method and incorporated (1.5 wt.%) in solvent free epoxy coatings. The obtained hydrotalcites were characterized using infrared spectroscopy, X-ray diffraction, scanning electron microscopy and zeta potential measurements. The solid suspensions in epoxy resin were characterized by rheology and Turbiscan. The corrosion protection performance of the epoxy coating containing hydrotalcites applied on carbon steel was evaluated by electrochemical impedance spectroscopy, salt spray test and adhesion measurement. It was shown that the BTSA and BZ were intercalated in hydrotalcite and their loading was about 22 wt.% and 27 wt.%, respectively. The presence of BZ modified hydrotalcite (HT-BZ) improved significantly the corrosion protection of solvent free epoxy coating. Corrosion protection performance of epoxy coating containing HT-BZ was higher than that of epoxy coating containing BTSA modified hydrotalcite (HT-BTSA). The corrosion protection performance of coatings appears to depend on the dispersion degree of hydrotalcite particles in the epoxy matrix and the solubility of organic inhibitor in the electrolyte.

1. Introduction

Organic coatings are widely used for corrosion protection of metals. Due to the environmental problems related to the use of volatile organic solvents, many researches focus on the implementation of solvent free organic coatings. Organic acids are used as corrosion inhibitors in industry for corrosion protection of copper, steel, aluminum alloys. These organic compounds have several molecular bonds containing nitrogen, sulphur and oxygen atoms through which they can be adsorbed on the metal surface [1–4]. Benzoic acid and its substituted compounds are widely used as corrosion inhibitors and their inhibition efficiencies depend on the nature of the substituent and the substrates [5–7]. Benzoate compounds are studied as corrosion inhibitors for steel, zinc, copper, copper alloys, aluminum and aluminum alloys. The influence of benzoate concentration, pH, and dissolved oxygen on the corrosion of iron was previously investigated. The inhibition effect of benzoate is based on the blocking of anodic surface sites by the inhibitor molecule [8–13].

Dicarboxylic acids like adipic, succinic acids have been studied as corrosion inhibitors in combination with Zn salts for carbon steel in NaCl solution and a high inhibition efficiency was achieved. It was shown that a protective film is formed on the metal surface consisting of a complex between Fe^{2+} cations and carboxylic acid and a precipitate of zinc hydroxyde $Zn(OH)_2$, [14,15]. Corrosion inhibitors based on succinic acid derivates are used in organic coatings such as 2-benzothiazolyl-succinic acid and amine salt of 2-benzothiazolyl-succinic acid [16].

Hydrotalcites have been used as conversion coatings for aluminum alloys and galvanized steel [17–21]. Protection performance and adhesion of organic coatings were improved with the presence of hydrotalcite layers.

Hydrotalcites due to their lamellar structure and their global positive charge can be used to trap anionic inhibitors and to avoid undesirable interactions between inhibitor and matrixes dur-

* Corresponding author at: Université de Mons (UMONS), Faculty of Engineering, Materials Science Department, 20 Place du Parc, Mons, Belgium.
E-mail address: marjorie.olivier@umons.ac.be (M.-G. Olivier).

http://dx.doi.org/10.1016/j.porgcoat.2016.08.021
0300-9440/

ing the crosslinking reactions. By using hydrotalcites as inhibitor nanoreservoirs, the release of inhibitor species can also be triggered by exchange with the chloride anions contained in the aggressive electrolyte. Recently, hydrotalcites are studied as nanocontainers of corrosion inhibitor in organic coatings and sol-gel coatings for corrosion protection of aluminum alloys [22–30]. Hydrotalcites intercalated with different inorganic and organic anions like divanadate, vanadate, molybdate, aminobenzoate, benzoate, benzotriazolate, ethyl xanthate and oxalate were prepared before assessment of their corrosion protection. The coatings doped with hydrotalcites intercalated with divanadate offer a self-healing effect and show higher corrosion protection performance than that of chromate-based systems [25,31]. Organo-modified hydrotalcites improved barrier properties of the coating. However, the water uptake process causes blistering of the film [26]. HTs can provide effective inhibition against filiform corrosion propagation on AA2024-T3 alloy coated by organic coatings [27,28]. The addition of HTs to sol–gel films improved the corrosion resistance of coated AA2024-T3 alloy evaluated by salt spray test [29].

Evaluation of protection performance of coatings containing hydrotalcite intercalated with benzotriazolate, ethyl xanthate and oxalate for corrosion protection of aluminum alloys highlighted the inhibition efficiency to be depending on the structure of the organic anion, increasing in the following sequence: ethyl xanthate < oxalate < benzotriazolate [28].

Hydrotalcites containing 2-mercaptobenzothiazolate and quinaldate were synthesized and incorporated in organic coatings for corrosion protection of AA2024 aluminum alloy. It was shown that inhibitive anions can be released from hydrotalcite and the coatings containing modified hydrotalcites have self-healing properties [32].

Organic coatings containing molybdate intercalated hydrotalcite and HT-MoO_4^{2-}/ZnO were also investigated on magnesium alloys. The results indicated that the MoO_4^{2-} anion may be released from hydrotalcite in NaCl solution by exchange reaction with chloride, whereas ZnO particles can attract negatively charged anions, leading to the formation of a reinforced layer on the surface of the magnesium alloy [33].

Even if many surveys are related to corrosion protection of aluminum alloys, few studies concern the assessment of the efficiency of hydrotalcites intercalated with corrosion inhibitors for the protection of carbon steel. Nevertheless, protection performance of alkyd coating containing hydrotalcite intercalated with vanadate was reported and compared with coatings containing ion exchange silica and $ZnCrO_4$. It was shown that the inhibitive efficiency of hydrotalcite intercalated with vanadate was lower than that of $ZnCrO_4$ [34].

Anticorrosion efficiency of benzoate intercalated Zn–Al hydrotalcite used as inhibitive species for carbon steel was previously studied. The results indicated that the benzoate anions release from hydrotalcite and are replaced by aggressive chloride anion adsorbed on the hydrotalcite. In a 3.5 wt.% NaCl solution, the direct addition of HT-benzoate decreases significantly the corrosion rate of carbon steel [35]. To date, no study has considered the corrosion protection obtained by addition of HT-benzoate in an organic coating applied on carbon steel.

In our previous works, hydrotalcites modified by 2-benzothiazolylthio-succinic acid inhibitor (HT-BTSA) were synthesized, incorporated in a solvent based epoxy coating and applied on carbon steel [36–38]. The obtained results proved that HT-BTSA improved corrosion protection, adhesion and resistance to cathodic disbonding of solvent based epoxy coatings.

In this work, hydrotalcites intercalated with two different corrosion inhibitors: 2-benzothiazolylthio-succinic acid and benzoate were prepared and incorporated in solvent free epoxy coatings applied on carbon steel. The effect of the modification of hydrotalcites by corrosion inhibitor on dispersion and stability of charged epoxy resin was studied and the protection performance of coatings was investigated.

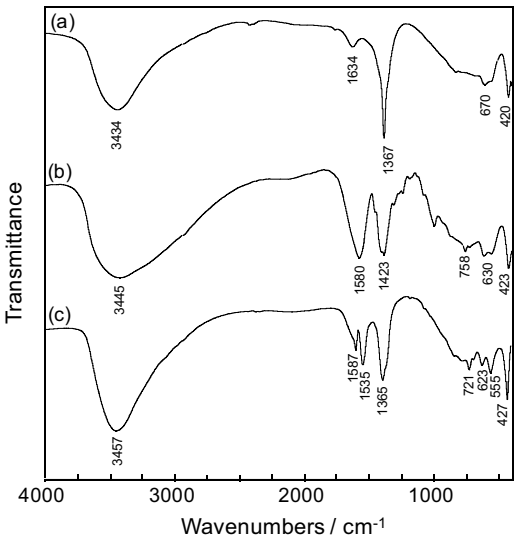

Fig. 1. FT-IR spectra of (a) hydrotalcite (HT); (b) hydrotalcite intercalated with 2-benzothiazolylthio-succinic acid (HT-BTSA) and (c) hydrotalcite intercalated with benzoate (HT-BZ).

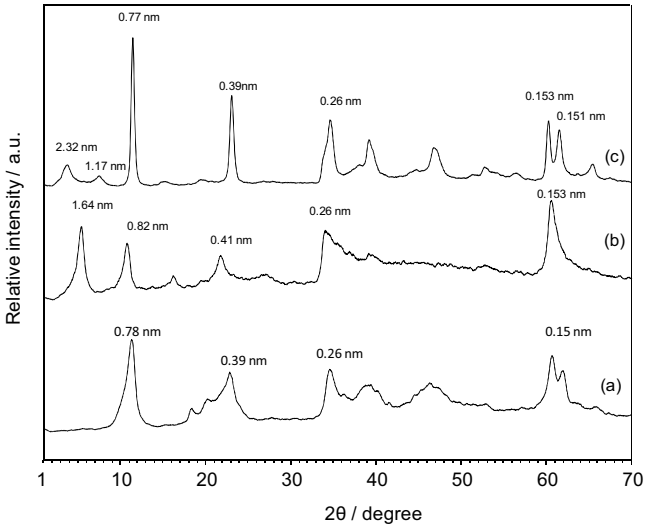

Fig. 2. XRD patterns of (a) HT; (b) HT-BTSA and (c) HT-BZ.

2. Experimental

2.1. Materials

Sodium hydroxide, zinc nitrate hexahydrate ($Zn(NO_3)_2{\cdot}6H_2O$), aluminum nitrate nonahydrate ($Al(NO_3)_3{\cdot}9H_2O$) were purchased from Sigma Aldrich. 2-benzothiazolylthio-succinic acid (BTSA) was obtained from Ciba Company and sodium benzoate (BZ) was purchased from VWR.

For the coatings, carbon steel sheets (150 mm × 10mm × 2 mm) were used as substrates. Sheets were polished with abrasive papers from grade 80 to 600 and cleaned with ethanol.

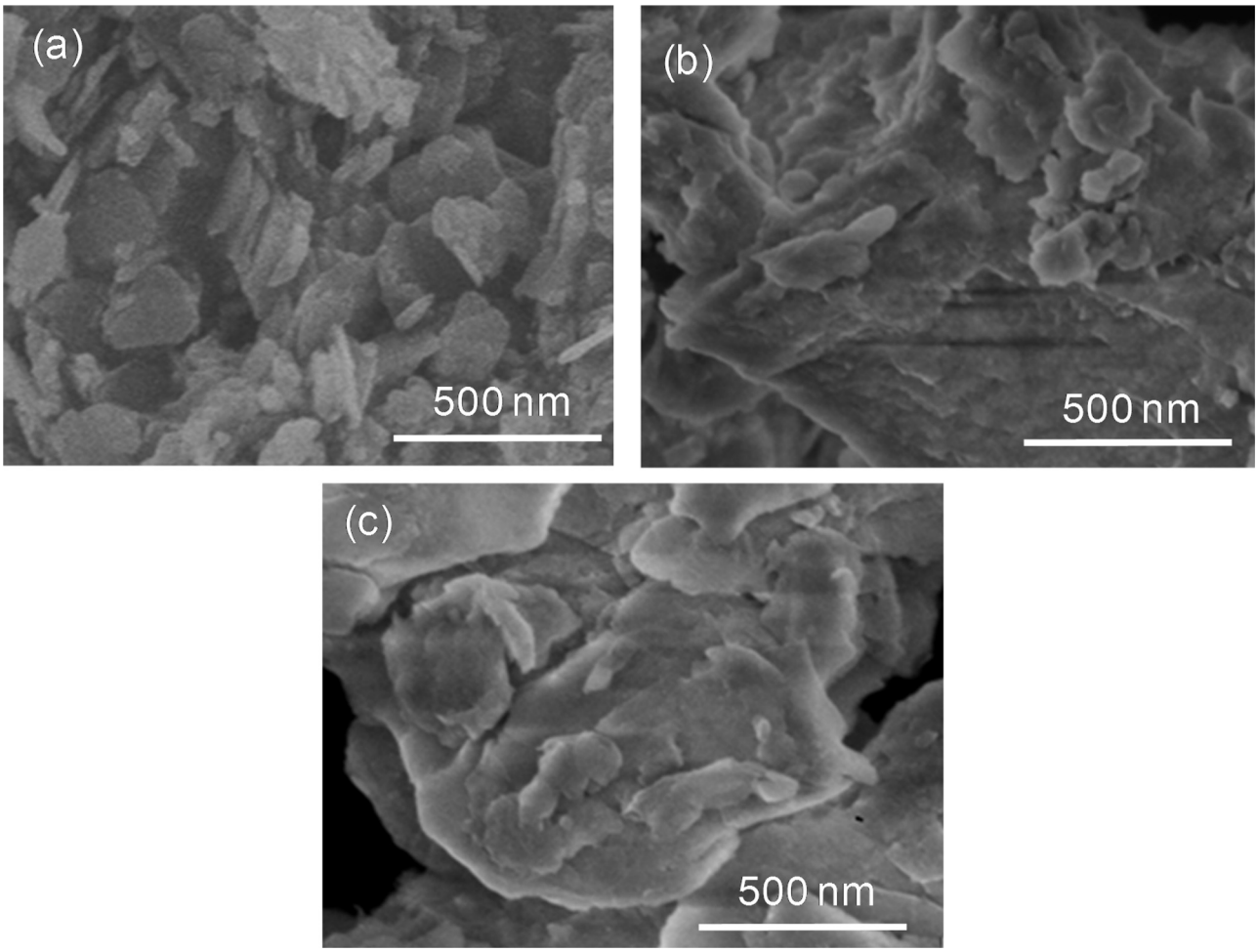

Fig. 3. SEM images of (a) HT; (b) HT-BTSA and (c) HT-BZ.

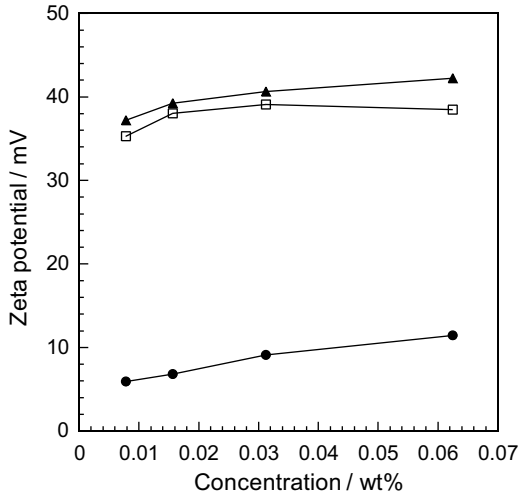

Fig. 4. Zeta potential of (□) HT; (●) HT-BTSA and (▲) HT-BZ at different concentrations.

2.2. Preparation of hydrotalcites

The zinc aluminum hydrotalcite (HT) was synthesized using the co-precipitation method [39]. The preparation was performed in a nitrogen atmosphere to exclude CO_2 which would lead to the incorporation of carbonate in the HT. A solution of 0.125 mol of $Zn(NO_3)_2{\cdot}6H_2O$ and 0.0625 mol of $Al(NO_3)_3{\cdot}9H_2O$ in 125 ml of degassed distilled water was added drop by drop over 1 h to a solution of 0.313 mol of NaOH in 145 ml of degassed distilled water. The pH of the solution was maintained at 8–10 by adding 1 M NaOH solution as needed. The resulting white precipitate was aged for 24 h at 65 °C, and then filtered until all of the supernatant liquid was removed. The sample was washed several times with large amounts of degassed distilled water and dried at 50 °C in a vacuum oven.

2.3. Preparation of hydrotalcites intercalated with inhibitors

2.3.1. Preparation of hydrotalcite intercalated with 2-benzothiazolylthio-succinic acid (HT-BTSA)

Hydrotalcites intercalated with BTSA (HT-BTSA) were prepared by the co-precipitation method [39] using the same procedure described for the preparation of net hydrotalcites. In that case, 0.313 mol of BTSA was added to the alkaline solution of $Zn(NO_3)_2{\cdot}6H_2O$ and $Al(NO_3)_3.9H_2O$. The solution was stirred vigorously under an inert nitrogen atmosphere and maintained at pH 8–10 before ageing and washing.

2.3.2. Preparation of hydrotalcite intercalated with benzoate (HT-BZ)

The hydrotalcites intercalated with benzoate were prepared following the same procedure as in Section 2.3.1. However, the resultant slurry was aged at 50 °C instead of 65 °C.

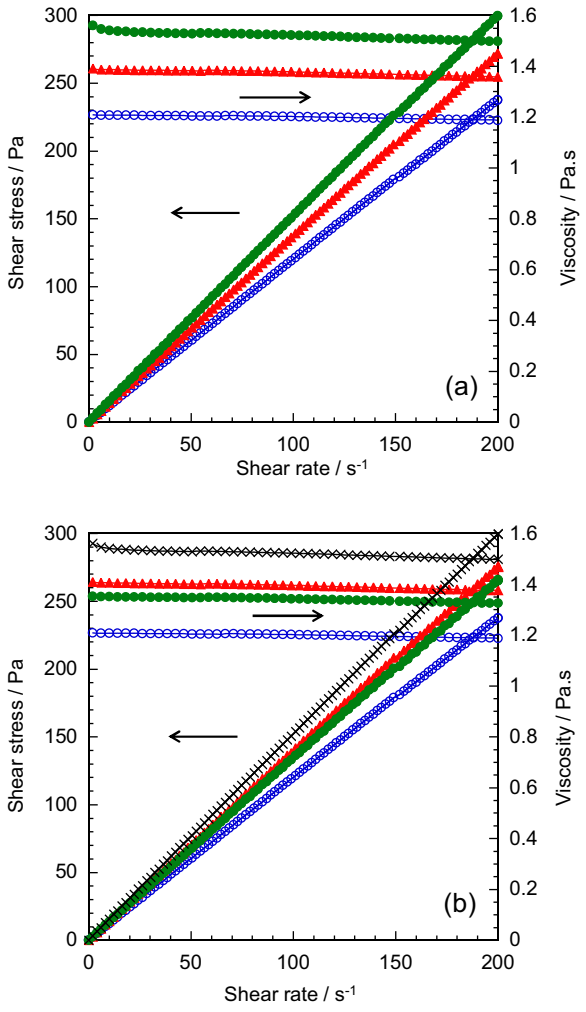

Fig. 5. Flow curves of epoxy resin containing (a) HT-BZ at (○) 0 wt.%; (▲) 1 wt.%; (●) 3 wt.% – (b) epoxy resin (○) and epoxy resin containing 3% (●) HT, (▲) HT-BTSA and (x) HT-BZ.

2.4. Coating preparation

The used solvent free epoxy coating was based on Epon 828 (Momentive) with equivalent weight of 185–192 g/eq and Ancamine 2753 (Air product) hardener with equivalent weight per active H of 153 g/eq.

Hydrotalcites were incorporated in the epoxy resin at a concentration of 1.5 wt.% and dispersed by magnetic stirring for 20 min and then sonicated with ultrasonic waves at a 35 kHz frequency for 15 min (5 times) and finally stirred for 24 h. The hardener was added to epoxy resin containing hydrotalcites just before application. The liquid paint was applied by spin coating at 1000 rpm for 10 s and dried at room temperature for 7 days. The dry film thickness was 40 ± 5 μm (measured with Minitest 600 Erichen digital meter).

2.5. Analytical characterization

Fourier transform infrared spectra were obtained using the KBr method on a Nexus 670 Nicolet spectrometer operated at 1 cm^{-1} resolution in the 400–4000 cm^{-1} region.

UV–vis spectra were obtained using UV–vis spectroscopy CINTRA 40, GBC.

X-ray diffraction measurements were performed with a Siemens diffractometer D5000 with Cu Kα X-Ray diffraction.

FE-SEM observations were carried out using a Hitachi SU8020 spectrometer.

2.6. Measurement of loading amount of BTSA and BZ in modified hydrotalcites

The loading amounts of BTSA or BZ in modified hydrotalcites were determined by UV–vis spectroscopy using the following method: 0.05 g of hydrotalcite was dissolved in 0.5 ml of 6 M HNO_3 solution contained in a 10 ml volumetric flask, the balance was filled with ethanol. The concentrations of BTSA or BZ in the resulting solutions were determined by monitoring the absorbance at λ_{max} = 283 nm (BTSA) and λ_{max} = 225 nm (BZ) by using UV–vis spectroscopy. The BTSA or BZ concentrations were calculated using regression analysis according to the standard curves obtained from a series of standard solutions of BTSA or BZ.

2.7. Zeta potential measurements of HT-BTSA and HT-BZ

The zeta potential measurements of the HT-BTSA and HT-BZ in distilled water were carried out using a MALVERN Zetasizer Nano ZS. The concentrations of suspended solids were adjusted to 0.01–0.06 wt.%.

2.8. Rheological characterization and suspension stability

Hydrotalcites were dispersed in epoxy resin by grinding for 30 min and then sonicated with a Hielscher UP100H sonicator with the power set to 16 W for 10 min and controlled in temperature by using tap water circulation.

The rheological behavior of pristine epoxy resin and epoxy resin containing HT-BTSA or HT-BZ at different concentrations (0.5 wt.%, 1 wt.% and 3 wt.%) was determined with an Anton Paar Modular Compact Rheometer MCR 302.

The flow curves were determined at 25 °C using the rheometer with parallel-plate mode (PP50). The shear rate was controlled from 0 to 200 s^{-1} for 600 s and the corresponding shear stress measured.

The stability measurements of the suspensions obtained by adding 1.5 wt.% of HT, HT-BTSA or HT-BZ in epoxy resin were carried out using a Turbiscan Lab^{Expert} at 30 °C. The suspensions were analyzed in a glass vial (7 cm in length) placed in a thermostated chamber and poured to 40 mm. The changes in the suspension stability were monitored for 4 days. The results are presented with time in the form of transmission and backscattering difference (delta), both expressed in%. The transmission and backscattering data are used for calculation of the stability coefficient TSI (Turbiscan Stability Index). This index is a key number related to the general behavior of the suspension. This index is very useful for the comparison of different samples. The TSI values change in the range from 0 (high stability) to 100 (very unstable behavior). The lower the TSI value is, the more stable the system is.

2.9. Electrochemical impedance measurement

Protection performance of coatings containing hydrotalcites was evaluated by electrochemical impedance measurements (EIS). A three-electrode cell was used with a large platinum counter electrode, an Ag/AgCl (sat. KCl) reference electrode and coated carbon steel samples as working electrode with an exposed area of 28 cm^2. The electrochemical impedance measurements were performed using a VMP3-BioLogic (Science Instruments) over a frequency range of 100 kHz to 10 mHz with six points per decade using a 30 mV peak-to-peak sinusoidal voltage. A 0.5 M NaCl solution was used as the electrolyte for the electrochemical tests. All the tests were performed at room temperature. Each experiment was done at least three times. The barrier properties and more particularly

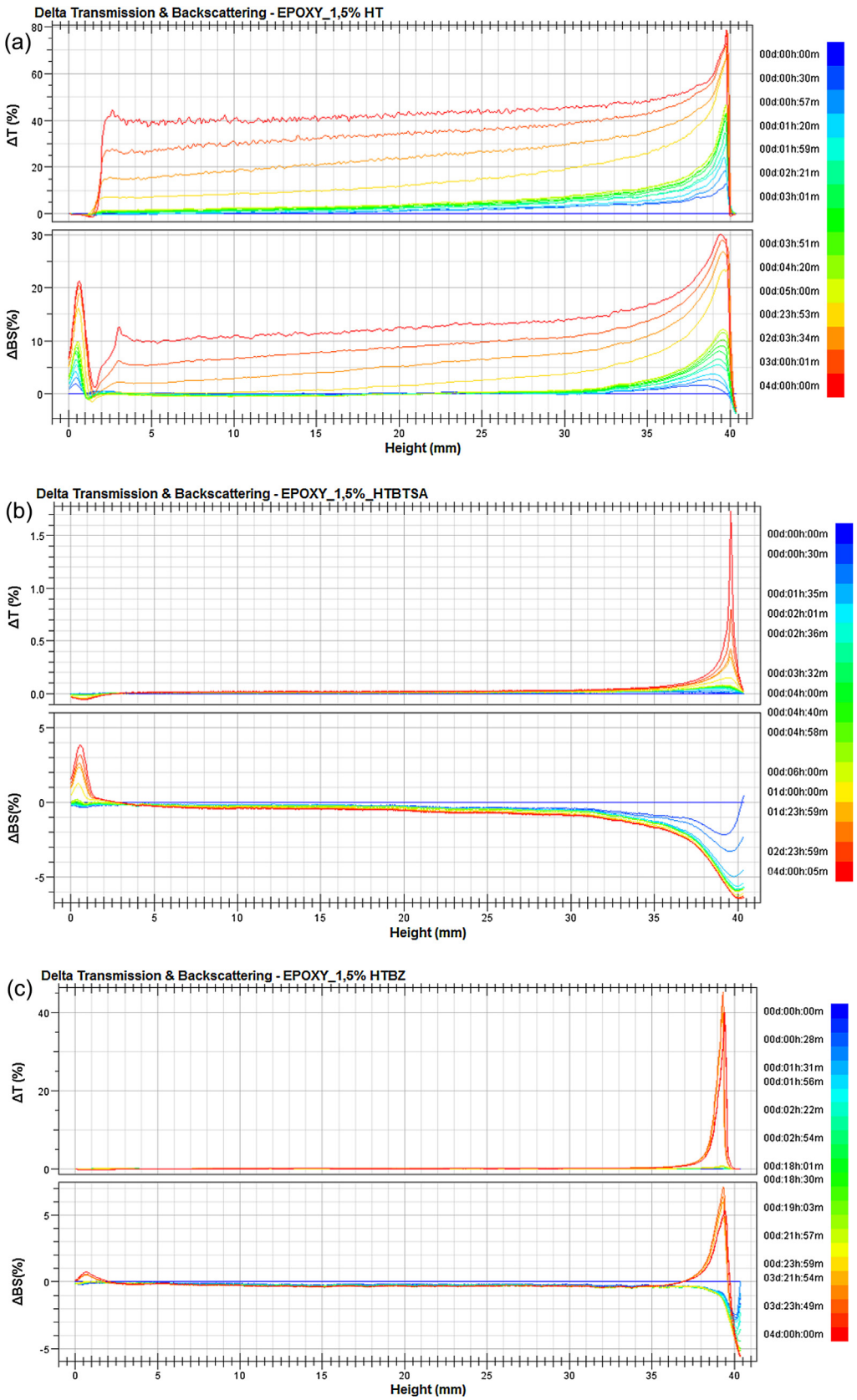

Fig. 6. Transmission and backscattering curves for epoxy resin containing 1.5 wt.% (a) HT, (b) HT-BTSA and (c) HT-BZ. Scan sequence varies from bottom to top of vial at the time of measurement.

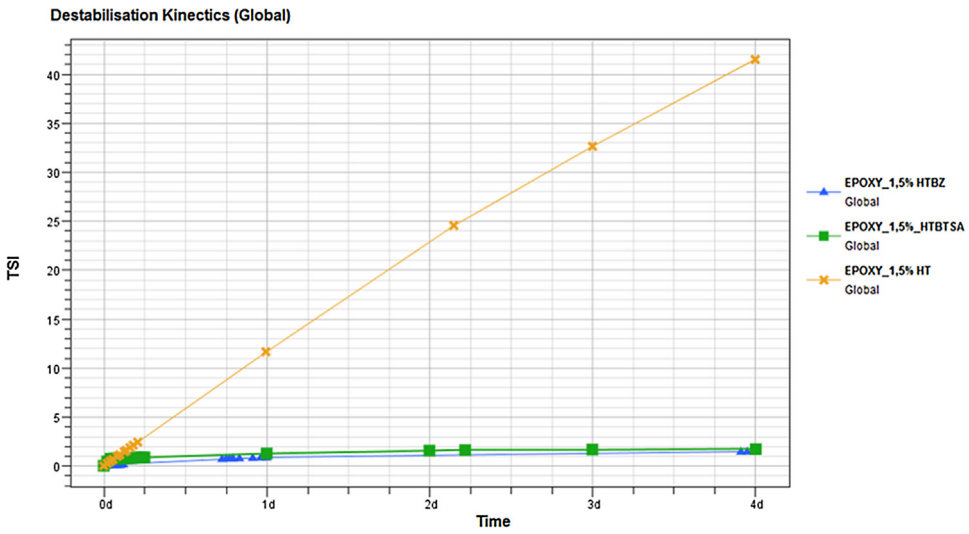

Fig. 7. Turbiscan Stability Index (TSI) of epoxy resin containing unmodified and modified hydrotalcites versus time.

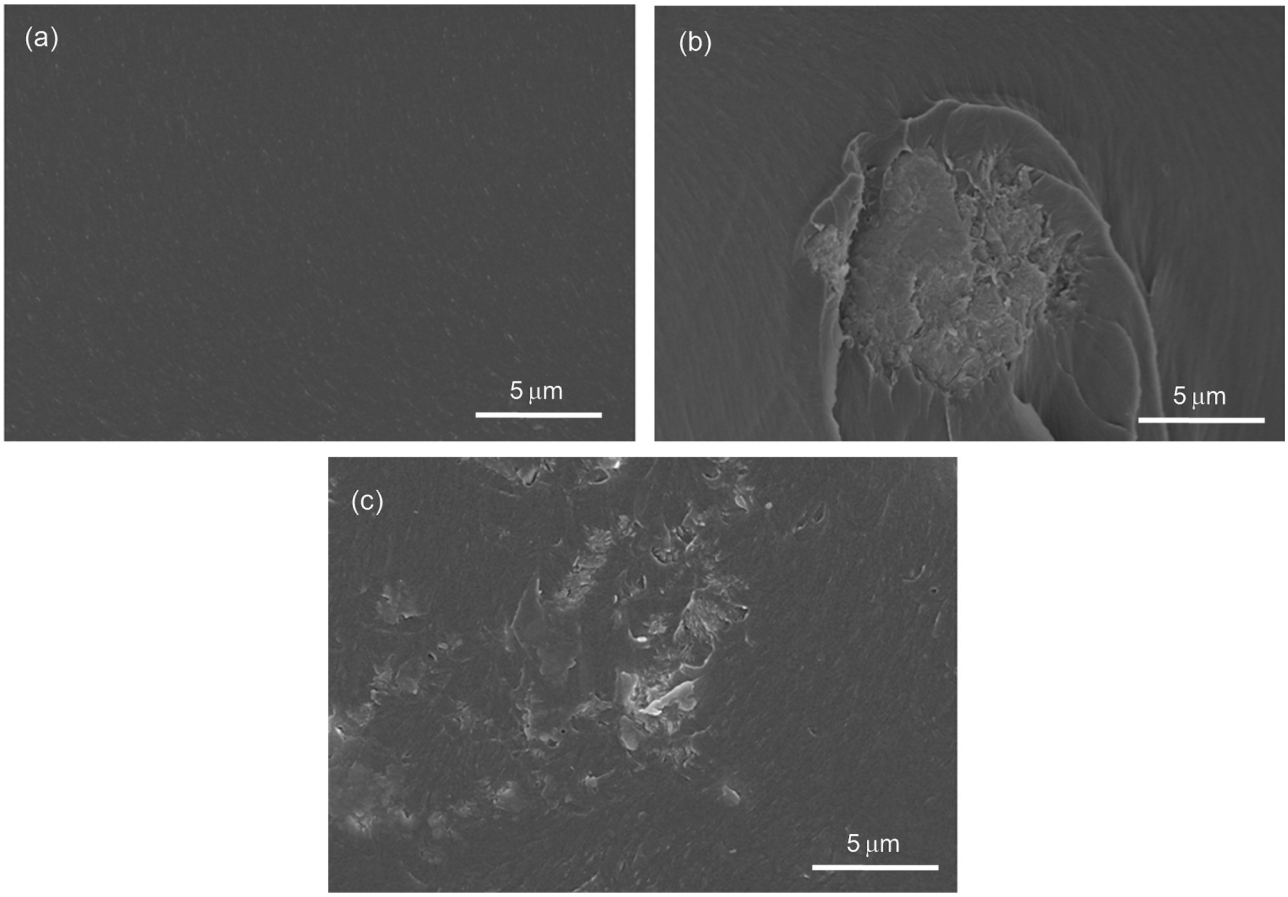

Fig. 8. SEM images of fracture surface (a) of epoxy coating; (b) epoxy coating containing 1.5 wt.% HT-BTSA and (c) epoxy coating containing 1.5 wt.% HT-BZ.

the film resistances of organic coatings were evaluated by using the Zfit software supplied by BioLogic which calculates this value from the demi-circle measured at high frequency in the Nyquist diagrams.

2.10. Salt spray test

Salt spray test was performed according to ASTM B117 using a Q-FOGCCT-600 chamber. The coated steels were scratched and placed in a salt spray chamber and the sample surfaces after testing were observed. Rusting and delamination degrees (mm) from the scribe were determined and compared. As the epoxy coating is transparent, the delamination degree can be observed and measured by considering the penetration distance of the electrolyte under the coating. This distance is measured perpendicularly to the scratch without removing the organic film from the test panel.

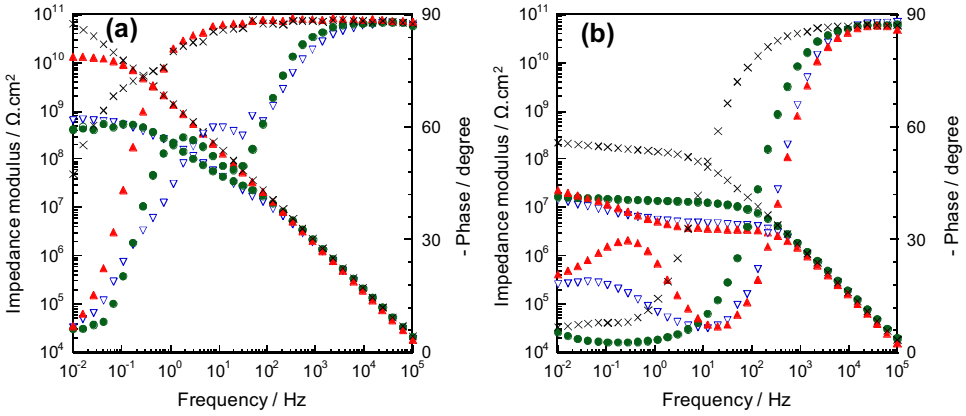

Fig. 9. Electrochemical impedance diagrams (Bode representation) obtained after (a) 2 h and (b) 42 days exposure to 0.5 M NaCl solution for the carbon steel covered by: (▽) pure epoxy coating, (●) epoxy coating containing 1.5 wt.% HT, (▲) epoxy coating containing 1.5 wt.% HT-BTSA and (x) epoxy coating containing 1.5 wt.% HT-BZ.

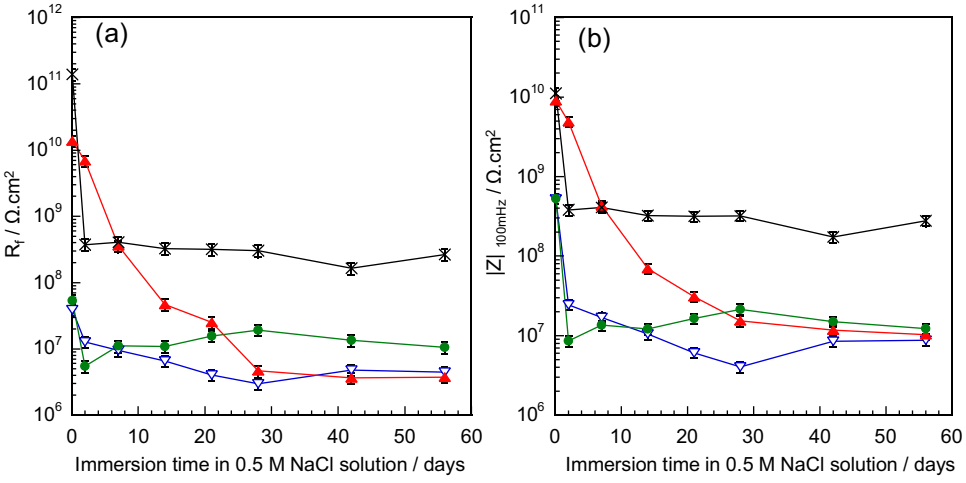

Fig. 10. R_f (a) et $|Z|_{100mHz}$ (b) versus immersion time in 0.5 M NaCl solution for the carbon steel covered by: (▽) pure epoxy coating, (●) epoxy coating containing 1.5 wt.% HT, (▲) epoxy coating containing 1.5 wt.% HT-BTSA, (x) epoxy coating containing 1.5 wt.% HT-BZ.

2.11. Adhesion test

The adhesion strength values of the coatings were measured according to ASTM D4541 using a PosiTest digital Pull-Off adhesion tester (DeFelsko) with 20 mm dollies. The dollies were glued on the surface of the epoxy coating using 2-part AralditTM Epoxy adhesive. The maximum force necessary to detach the coating from the steel plate was recorded as a measure of the bond strength between the coating and the substrate. All the tests were performed on three samples at room temperature.

3. Results and discussion

3.1. Characterization of HT-BZ and HT-BTSA

Chemical compositions and inhibitor content of HT-BZ and HT-BTSA are summarized in Table 1. The experimental atomic ratio of Zn/Al for HT-BZ and HT-BTSA was 2.13/1 and 2.41/1 respectively. The BZ loading in HT-BZ was 27.0 wt.% and the BTSA loading in HT-BTSA 21.9 wt.%. These loadings are significant and for the HT-BZ in good agreement with the result obtained by Wang et al. [35].

The FT-IR spectra of HT, HT-BZ and HT-BTSA are presented in Fig. 1.

In FT-IR spectrum of HT, bands at 420 cm^{-1}, 670 cm^{-1}, 1367 cm^{-1} and 1634 cm^{-1} can be observed. They are attributed to Zn-O, Al-O vibrations, NO_3^- group and water molecules in the interlayer domain, respectively [40].

The FT-IR spectrum of HT-BTSA (Fig. 1b) displays the characteristic bands of Zn-O and Al-O at 423 cm^{-1} and 630 cm^{-1}. The bands at 1580 cm^{-1} and 1423 cm^{-1} are related to the COO^- group [41]. This result indicates the presence of BTSA in the form of carboxylate anion in the hydrotalcite structure.

The FT-IR spectrum of HT-BZ (Fig. 1c) has characteristic peaks of Zn-O, Al-O and NO_3^- group at 427 cm^{-1}, 623 cm^{-1} and 1365 cm^{-1} [40]. The bands at 1587 cm^{-1} and 1535 cm^{-1} characteristic of COO^- group are also observed for HT-BZ [41,35]. The results indicate that benzoate is well present in the modified hydrotalcites. Whatever the considered modified hydrotalcite, the characteristic band of NO_3^- anion is still observed meaning that the anionic exchange is partial. The X-ray diffraction patterns of synthesized HT, HT-BTSA and HT-BZ are shown in Fig. 2. The XRD patterns of synthesized HT, HT-BTSA and HT-BZ are representative of layered materials.

The XRD pattern of HT shows the (003) reflection corresponding to the basal spacing of 0.78 nm. For HT-BTSA basal spacing increased to 1.64 nm and 0.82 nm. The increase of d-spacing value at 1.64 nm confirms the intercalation of BTSA in the interlayer domain of hydrotalcite. The XRD pattern of HT-BZ displays the (003) reflection corresponding to the basal spacing of 2.32 nm, 1.17 nm and 0.77 nm. The two first peaks correspond to higher values of d-spacing than the ones of HT and HT-BTSA confirming that benzoate is intercalated in the interlayer region of hydrotalcite. The higher basal

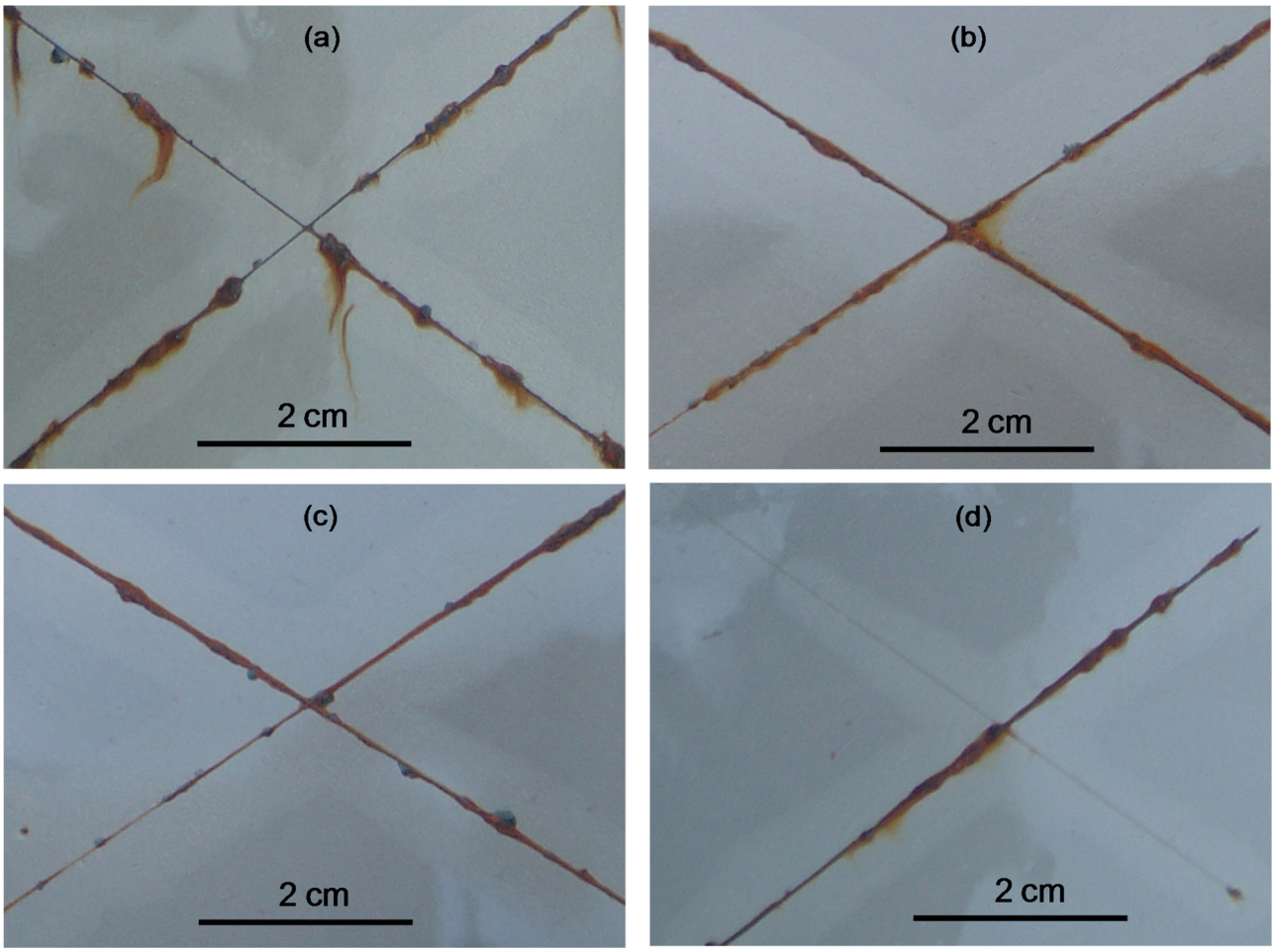

Fig. 11. Photographs after 96 h exposure to salt spray test of (a) pure epoxy coating, (b) epoxy coating containing 1.5 wt.% HT, (c) epoxy coating containing 1.5 wt.% HT-BTSA and (d) epoxy coating containing 1.5 wt.% HT-BZ.

Table 1
Elemental analysis data of HT-BZ and HT-BTSA.

Sample	Content (wt.%)		Atomic ratio Zn/Al	Inhibitor content (wt.%)	
	Zn	Al		BZ	BTSA
HT-BZ	34.84	6.78	2.13	27.0	
HT-BTSA	28.33	4.86	2.41		21.9

spacing of HT-BZ by comparison with HT-BTSA can be explained by the higher content of BZ in modified hydrotalcite or the orientation of BZ molecules in hydrotalcite structure. However, for all the synthetized hydrotalcites, the characteristic d-spacing around 0.77 nm is observed and related to the nitrate anions present in the d-spacing. These results are in good agreement with the FT-IR data. Despite the large amount of inhibitive species measured by UV–vis spectroscopy, NO_3^- anions are not completely replaced in the structure of the modified hydrotalcites.

SEM images of HT, HT-BTSA and HT-BZ are shown in Fig. 3. All samples show the typical plate-like morphology of hydrotalcite with particle sizes in the range from 50 nm to 200 nm. HT-BTSA and HT-BZ have similar morphology but the individual crystals can be less distinguished than for HT.

The surface charge properties of HT, HT-BTSA and HT-BZ were estimated by zeta potential measurements in distilled water at neutral pH. The zeta potential of HT, HT-BTSA and HT-BZ measured at different concentrations are presented in Fig. 4. It can be observed that the zeta potentials of HT and HT-BZ are positive and higher than 30 mV. While the zeta potentials of HT-BTSA are very low, lower than 10 mV. These results indicate that the suspensions of HT and HT-BZ are much more stable in neutral aqueous solution than the suspensions of HT-BTSA. The low value of zeta potential of HT-BTSA can be explained by the adsorption of BTSA on the hydrotalcite surface and the solubility difference between the two inhibitive species. Indeed, the benzoate as well as the nitrate are soluble in water. The solubility of benzoate (630 g/L at 20 °C) is very high compared to the one of BTSA (0.27 g/L). During immersion in distilled water, the benzoate, present at the external surface of hydrotalcite, is soluble, showing a negative charge due to its carboxylate group and is desorbed as in the case of the nitrate anions. Due to its very low solubility, the BTSA might remain at the surface and reduce the global positive charge of hydrotalcites.

3.2. Dispersion of hydrotalcites in solvent free epoxy resin

3.2.1. Rheological characterization

Flow curves measured in a range of shear rates of 0–200 s^{-1} were carried out to investigate the rheological properties of epoxy resins containing hydrotalcites. The flow curves of epoxy resin containing HT-BZ at different concentrations (0, 1, 3%) are presented in Fig. 5a. In this concentration range, a Newtonian behavior is observed whatever the investigated system, meaning there is no interaction between the platelets at low shear rate and no shear-thinning behavior is observed when the shear rate increases. As a consequence, the yield stress is equal to zero and no orientation in the shear direction is highlighted. This behavior seems to indicate that the hydrotalcites are well dispersed in the coatings in this concentration range. As shown in Fig. 5a, the incorporation of hydrotalcite provokes a viscosity rise as shown for the incorporation of HT-BZ. This increase can be explained by the higher amount of insoluble matter in the epoxy binder. The same behavior is observed for HT and HT-BTSA (not shown here). In order to compare the different synthetized hydrotalcites, their rheological behavior is reported in Fig. 5b for a concentration of 3 wt.%. It is worth nothing that Newtonian viscosity is similar for HT and HT-BTSA but is higher when the same concentration of HT-BZ is incorporated in the epoxy coatings: 1.32 Pa s, 1.38 Pa s and 1.5 Pa s respectively. This behavior can be attributed to a better dispersion of HT-BZ in the epoxy coatings. As suggested by these measurements, the particle size is probably lower after dispersion in the epoxy resin and therefore the particle number higher at the same concentration.

3.2.2. Suspension stability

The suspensions were characterized by Turbiscan equipment. A stable suspension is characterized by a stable value of the transmission and the backscattering intensities over the sample height with time. The transmission and backscattering profiles of the epoxy resin containing 1.5 wt.% of HT, HT-BTSA and HT-BZ are shown in Fig. 6. In the case of the epoxy resin (Fig. 6a) containing unmodified hydrotalcites, the difference in or delta transmission increases significantly with time over the whole height of the sample, reaching a value of 40% after 4 days. This observation is representative for an unstable behavior with a clarification of the solution probably due to the formation of soft and large aggregates over the whole height of the sample. A different behavior is observed when the hydrotalcites are modified by inhibitive species. In particular, the transmission signals of the modified hydrotalcites are close to the baseline during the entire time of analysis. The occurrence of the clarifying process in suspension is underlined by the presence of a transmission peak located at the top surface for both samples. In order to obtain more information on the nanoparticle migration, the backscattering signal is useful. The presence of peaks in the backscattering curves indicates sedimentation, the sediment thickness being equal to the width of this peak at the bottom of the vial. As observed in the backscattering profile (Fig. 6b), a sediment of small intensity (3 mm) is detected for the epoxy resin containing HT-BTSA after 6 h. In contrast, for the epoxy resin containing HT-BZ, a weak sedimentation starts to appear after 4 days and the migration of particles concerns mainly the top surface even after this time (Fig. 6c).

The global stabilities of the suspension were characterized by the TSI value versus time (Fig. 7). In the light of these results, the epoxy resins containing modified hydrotalcites are very stable compared to the unmodified one. The TSI values after 1 day are 11.7, 1.3 and 0.8 for the HT, HT-BTSA and HT-BZ respectively. The modification of hydrotalcites by an organic inhibitor appears to improve the suspension stability in the epoxy resin. The more stable suspensions were obtained after benzoate modification. In organic medium, the inhibitive species which are organic inhibitors increase the hydrophobicity of the hydrotalcite surfaces, improves the compatibility with the organic matrix and favors the dispersion in the organic resin.

3.2.3. Coating morphology

In order to confirm the formerly observed difference in results between HT-BZ and HT-BTSA, the dispersion degree of HT-BZ and HT-BTSA in solvent free epoxy coatings was also investigated by SEM trying to focus on the possible formation of aggregates or defects. Fig. 8 shows SEM images of fracture surface of solvent free epoxy coatings at the same magnification: the clear epoxy coating and epoxy coating containing 1.5 wt.% HT-BZ and HT-BTSA, respectively. For the clear epoxy coating, as expected, the surface is uniform and smooth whatever the analyzed surface. Although the number of detected aggregates is small, for epoxy coatings containing HT-BTSA, agglomeration of particles can be clearly observed at certain places. The size of these aggregates can reach several microns. For epoxy coatings containing 1.5 wt.% HT-BZ, the presence of hydrotalcite structures, well dispersed in the epoxy matrix, is observed even though small aggregates in the μ-range can still be identified. These results are in good agreement with the information obtained from the flow curves of epoxy coatings and Turbiscan data.

3.3. Corrosion protection of coatings

3.3.1. Electrochemical impedance measurement

Barrier protection of solvent free epoxy coating and epoxy coatings containing hydrotalcites was evaluated by electrochemical impedance spectroscopy. The impedance diagrams of coatings obtained after 2 h and 42 days of exposure to 0.5 M NaCl solution are presented in Fig. 9. For the impedance diagrams of organic coatings, the high-frequency part is related to the organic coating while the low frequency part gives the information about the reactions occurring on the metal through defects and pores in the coating [42,43].

At the beginning of exposure, the impedance diagrams of the coatings containing modified hydrotalcites are characterized by one time constant and the impedance modulus at low frequencies were high and superior to 10^{10} Ω cm^2. The impedance diagrams of the clear epoxy coating and containing unmodified hydrotalcites already seem to present two time constants and show values of the modulus at low frequencies which are two orders of magnitude lower. This behavior can be expected for a clear coat because as shown by different authors the nanoparticles such as pigments can fill the microdefects present in clear organic coating if they are well dispersed and compatible with the organic matrix [44–46]. The inorganic nature of the unmodified hydrotalcite (HT) and the formation of aggregates observed in the matrix can explain the low initial barrier protection of this system. After 42 days of exposure to a 0.5 M NaCl solution, the impedance modulus of the coatings decreased, the impedance modulus of the coating containing HT-BZ remaining the highest and the values of the other coatings being close.

According to literature, the impedance modulus at low frequency, between 1 and 0.01 Hz, is an appropriate parameter for characterization of corrosion protection of coatings [47–50]. From impedance diagrams film resistance, R_f and impedance modulus at 100 mHz, $|Z|_{100mHz}$ were estimated to evaluate the protection performance of coatings. The R_f value was determined considering the time constant at high frequency. Fig. 10 presents the variation of R_f and $|Z|_{100mHz}$ during immersion time in 0.5 M NaCl solution for the carbon steel covered by solvent free epoxy coatings without and with hydrotalcites. The variations of $|Z|_{100mHz}$ values of all coatings were similar to the variations of R_f values. These dia-

grams obtained on these not previously scratched samples cannot be used to estimate the inhibitive protection given by the inhibitive species in hydrotalcite intercalated position due to the significant contribution of the organic coatings in the protective system. Nevertheless, these measurements can be very useful to evaluate the impact of dispersion stability on the barrier properties of coatings and the compatibility of modified hydrotalcites with the organic matrix. After 2 h of immersion, the R_f values of all coatings were quite high and the values of coatings containing HT-BTSA and HT-BZ were much higher than the one of pure epoxy coating and epoxy coating containing HT. After the first 2 days of immersion the R_f values of all coatings decreased rapidly. When immersion time increases, R_f values of pure epoxy coating and epoxy coating containing HT-BTSA continued to decrease, while R_f values of epoxy coating containing HT and epoxy coating containing HT-BZ remained stable. The decrease of R_f values was attributed to the penetration of water and electrolyte in the coatings. After 21 days of exposure the R_f values of epoxy coating containing HT-BZ and HT-BTSA still remained higher than the one of pure epoxy coating and epoxy coating containing HT. However, after 56 days of exposure, the R_f values of epoxy coatings containing HT-BZ remained quite high ($>10^8\ \Omega\ cm^2$) and much higher (10 times) compared to the other coatings. The R_f values of epoxy coating containing HT-BTSA decreased progressively but finally reached the one of pure epoxy coating and epoxy coating containing HT. These results indicate that the presence of HT-BZ improved significantly the barrier properties of epoxy coating, while HT-BTSA delayed their loss but reached after a long immersion period the same value than the pure epoxy one. Even if some aggregates can be detected by SEM-FEG, the EIS results confirm that the incorporation of hydrotalcite doesn't affect negatively the barrier performance of the coating. Due to the good dispersion of organically modified hydrotalcites in the organic coating, the decrease of the film resistance is delayed for HT-BTSA or this resistance is stabilized at a higher value when hydrotalcites are modified by benzoate.

3.3.2. Salt spray test

The corrosion resistance of carbon steel covered with a pure epoxy coating and epoxy coatings containing hydrotalcites was also evaluated by accelerated corrosion tests on scratched samples. The photographs of samples after 96 h exposure to salt spray test are shown in Fig. 11. The evaluation of the rusting and delamination degrees of coatings were presented in Table 2 after 96 h of exposure to salt spray test. For a pure epoxy coating, the accumulation of corrosion products is observed in the scratches. For epoxy coatings containing hydrotalcites, corrosion products are also formed but the corrosion degree is lower compared to a pure epoxy coating. The rust creepage from scribe of the pure epoxy coating was higher than that of epoxy coatings containing hydrotalcites. The rust creepage from scribe was the lowest for epoxy coating containing HT-BZ. The film delamination from scribe of pure epoxy coating was 2.7 mm. By comparison with pure epoxy coating, epoxy coating containing HT exhibits higher delamination degree and the epoxy coating containing HT-BZ and HT-BTSA have lower film delamination from scribe. The delamination degree was lowest for epoxy coatings containing HT-BZ (1.8 mm) after 96 h of exposure to salt spray test.

The salt spray test results indicate that the presence of HT, HT-BTSA and HT-BZ improves the corrosion resistance of the epoxy coating, HT-BZ providing the highest protection. These results prove the inhibitory action of BTSA and BZ at the interface coating/metal and confirm that the inhibition effect of HT-BZ was higher than HT-BTSA. This behavior can be explained by the low solubility of benzoate in water electrolyte which is probably leached in higher amount in the scratched area and can play this inhibitive action, limiting the corrosion extent.

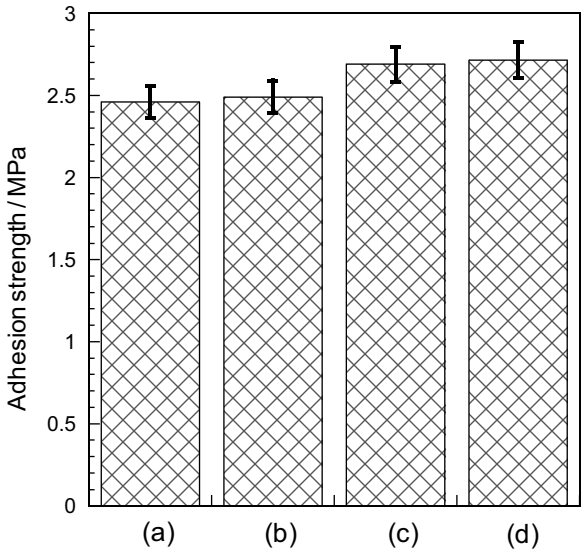

Fig. 12. Adhesion strength of (a) pure epoxy coating, (b) epoxy coating containing 1.5 wt.% HT, (c) epoxy coating containing 1.5 wt.% HT-BTSA, (d) epoxy coating containing 1.5 wt.% HT-BZ.

3.3.3. Adhesion measurement

Adhesion is the important property of organic coatings [51,52]. The adhesion strengths of coatings are shown in Fig. 12. It is observed that the adhesion strength of the pure epoxy coating was 2.4 MPa. The adhesion strength of epoxy coating containing HT is close to the one of pure epoxy coating. The adhesion strengths of epoxy coating containing HT-BTSA or HT-BZ are very close and higher than the one of pure epoxy coating. A similar result was obtained for the solvent based epoxy coatings [38]. The increase of the adhesion properties after incorporation of organically modified hydrotalcites can be explained by the presence of OH group on the nanoreservoirs, this group having a high affinity for the native oxide layer formed on the metallic substrate in short contact with the atmosphere before application of the organic coating. This behavior can also be attributed to the possible adsorption of inhibitive species on the metallic surface coming from the external surface of hydrotalcites. Due to the good dispersion of the modified nanoreservoirs, the number of bonds which can be formed with the carbon steel substrate raise when the hydrotalcites are modified. These results are in good agreement with the salt spray test.

4. Conclusions

Hydrotalcites intercalated with 2-benzothiazolythio-succinic acid and benzoate using the coprecipitation method were successfully synthesized and added in a solvent free epoxy coating. Rheological characterization, Turbiscan data and SEM analysis highlighted that the modification of hydrotalcites by organic inhibitive species enables to improve the particle dispersion in the epoxy resin. The most stable suspensions were obtained after benzoate incorporation. The presence of HT-BZ at a concentration of 1.5 wt.% significantly improved the barrier properties of solvent free epoxy coatings applied on carbon steel. The adhesion of epoxy coatings was slightly enhanced with the presence of HT-BTSA and HT-BZ. When the scratched samples are exposed to salt spray, the extent of the corrosion is reduced when inhibitive species are present in the hydrotalcite structure. This effect is more

Table 2
Salt fog test results according to ISO 4628.

Sample	Rusting degree (mm)	Delamination degree (mm)
Solvent free epoxy coating	0.72	2.7
Solvent free epoxy coating containing 1.5 wt% HT	0.60	3.6
Solvent free epoxy coating containing 1.5 wt% HT-BTSA	0.50	2.4
Solvent free epoxy coating containing 1.5 wt% HT-BZ	0.31	1.8

pronounced for benzoate and is attributed to its high leaching in aqueous electrolyte.

Acknowledgments

The authors gratefully acknowledge the financially support of Vietnam National Foundation for Science and Technology Development (NAFOSTED) under grant number 104.01-2012.15 and Académie de Recherche et d'Enseignement Supérieur (ARES) through Development Cooperation (PRD-CUD) project between Vietnam and Belgium. They also thank Marc Poorteman (UMONS) for his advice in dispersion stability.

References

[1] E. Rocca, J. Steinmetz, Corros. Sci. 43 (2001) 891–902.
[2] N.D. Nama, Q.V. Bui, M. Mathesh, M.Y.J. Tan, M. Forsyth, Corros. Sci. 76 (2013) 257–266.
[3] G. Hefter, N. North, S. Tan, Corrosion 53 (1997) 657–667.
[4] U. Rammelt, S. Kohler, G. Reinhard, Electrochim. Acta 53 (2008) 6968–6972.
[5] Z. Chen, L. Huang, G. Zhang, Y. Qiu, X. Guo, Corros. Sci. 65 (2012) 214–222.
[6] M. Finsgar, I. Milosev, Corros. Sci. 52 (2010) 2737–2749.
[7] S. Zor, Turk. J. Chem. 26 (2002) 403–408.
[8] U. Rammelt, S. Koehler, G. Reinhard, Corros. Sci. 50 (2008) 1659–1663.
[9] G.T. Hefter, N.A. North, S.H. Tan, Corros. Eng. 53 (1997) 657–667.
[10] I.A. Raspini, Corros. Sci. 49 (1993) 821–828.
[11] D.E. Davies, Q.J. Slaiman, Corros. Sci. 13 (1997) 891–896.
[12] G. Blustein, C.F. Zinola, J. Colloid Interface Sci. 278 (2004) 393–403.
[13] W.B. Wan Nik, O. Sulaiman, S.G. Eng Giap, R. Rosliza, Int. J. Technol. 1 (2010) 20–28.
[14] M. Manivannan, S. Rajendran, Res. J. Chem. Sci. 1 (8) (2011) 42–48.
[15] G.R.H. Florence, A.N. Anthony, J.W. Sahayaraj, S. Rajendran, Indian J. Chem. Technol. 12 (2012) 472–476.
[16] A. Braig, I. Sekine Ed, Electrochem. Soc. Corros. Div. (1998) 18–30.
[17] R.B. Leggat, S.A. Taylor, S.R. Taylor, Colloids Surf. A: Physicochem. Eng. Aspects 210 (2002) 69–81.
[18] J.K. Lin, C.L. Hsia, J.Y. Uan, Scr. Mater. 56 (2007) 927–930.
[19] R.G. Buchheit, S.B. Mamidipally, P. Schmutz, H. Guan, Corrosion 58 (2002) 3–14.
[20] F. Zhang, M. Sun, S. Xu, L. Zhao, B. Zhang, Chem. Eng. J. 141 (2008) 362–367.
[21] W. Zhang, R.G. Buchheit, Corrosion 58 (2002) 591–600.
[22] A.L.T. Thuilliez, C.T. Guého, J. Cellier, H.H. Bruening, F. Leroux, Prog. Org. Coat. 64 (2009) 182–192.
[23] J. Tedim, A. Kuznetsova, A.N. Salak, F. Montemor, D. Snihirova, M. Pilz, M.L. Zheludkevich, M.G.S. Ferreira, Corros. Sci. 55 (2012) 1–4.
[24] M.L. Zheludkevich, S.K. Poznyak, L.M. Rodrigues, D. Raps, T. Hack, L.F. Dick, T. Nunes, M.G.S. Ferreira, Corros. Sci. 52 (2010) 602–611.
[25] T. Stimpfling, F. Leroux, H.H. Bruening, Colloids Surf. A: Physicochem. Eng. Aspects 458 (2014) 147–154.
[26] J. Liu, Y. Zhang, M. Yu, S. Li, B. Xue, X. Yin, Prog. Org. Coat. 81 (2015) 93–100.
[27] H.N. McMurray, G. Williams, Corrosion 60 (2004) 219–228.
[28] G. Williams, H.N. McMurray, Electrochem. Solid State Lett. 7 (2004) B13–B15.
[29] D. Álvarez, A. Collazo, M. Hernández, X.R. Nóvoa, C. Pérez, Prog. Org. Coat. 68 (2010) 91–99.
[30] J.M. Vega, N. Granizo, D. dela Fuente, J. Simancas, M. Morcillo, Prog. Org. Coat. 70 (2011) 213–219.
[31] S. Chrisanti, K.A. Ralston, R.C. Buchheit, Corros. Sci. Technol. 7 (4) (2008) 212–218.
[32] S.K. Poznyak, J. Tedim, L.M. Rodrigues, A.N. Salak, M.L. Zheludkevich, L.F.P. Dick, M.G.S. Ferreira, ACS Appl. Mater Interfaces 1 (10) (2009) 2353–2362.
[33] X. Yu, J. Wang, M. Zhang, L. Yang, J. Li, P. Yang, D. Cao, Surf. Coat. Technol. 302 (3-4) (2008) 250–255.
[34] B. Chico, J. Simancas, J.M. Vega, N. Granizo, I. Díaz, D. de la Fuente, M. Morcillo, Prog. Org. Coat. 61 (2008) 283–290.
[35] Y. Wang, D. Zhang, Mater. Res. Bull. 46 (2011) 1963–1968.
[36] T.T.X. Hang, T.A. Truc, N.T. Duong, N. Pébère, M.G. Olivier, Prog. Org. Coat. 74 (2012) 343–348.
[37] T.T.X. Hang, T.A. Truc, N.T. Duong, P.G. Vu, T. Hoang, Appl. Clay Sci. 67-68 (2012) 18–25.
[38] T.T.X. Hang, N.T. Duong, T.A. Truc, T. Hoang, D.T.M. Thanh, S. Daopiset, A. Boonplean, J. Coat. Technol. Res. 12 (2015) 375–383.
[39] C. Nyambo, D. Chen, S. Su, C.A. Wilkie, Polym. Degrad. Stab. 94 (2009) 496–505.
[40] Z.P. Xu, P.S. Braterman, Appl. Clay Sci. 48 (2010) 235–242.
[41] W.W. Simons, Sadtler Research Laboratories, Inc., The Sadler Handbook of Infrared Spectra, Pennsylvania, 1978.
[42] L. Beaunier, I. Epelboin, J.C. Lestrade, H. Takenouti, Surf. Technol. 41 (1976) 237.
[43] N. Pébère, T. Picaud, M. Duprat, F. Dabosi, Corros. Sci. 29 (1989) l073.
[44] F. Deflorian, S. Rossi, M. Fedel, C. Motte, Prog. Org. Coat. 69 (2010) 158–166.
[45] M.F. Montemor, D.V. Snihirova, M.G. Taryba, S.V. Lamaka, I.A. Kartsonakis, A.C. Balaskas, G.C. Kordas, J. Tedim, A. Kuznetsova, M.L. Zheludkevich, M.G.S. Ferreira, Electrochim. Acta 60 (2012) 31–40.
[46] K. Sh. Ammar, B. Ramesh, S. Vengadaesvaran, A.K. Ramesh, Arof. Prog. Org. Coat. 92 (2016) 54–65.
[47] J. Kittel, N. Celati, M. Keddam, H. Takenouti, Prog. Org Coat. 46 (2003) 135–147.
[48] G.P. Bierwagen, D. Tallman, J. Li, L. He, C. Jeffcoate, Prog. Org. Coat. 46 (2003) 148–158.
[49] R.L. De Rosa, D.A. Earl, G.P. Bierwagen, Corros. Sci. 44 (2002) 1607–1620.
[50] B.R. Hinderliter, S.G. Croll, D.E. Tallman, Q. Su, G.P. Bierwagen, Electrochim. Acta 51 (2006) 4505–4515.
[51] T.R. Bullett, J.L. Prosser, Prog. Org. Coat. 1 (1972) 45–71.
[52] W. Funke, JOCCA 68 (1985) 229–232.